© *1998 The Chemical Society of Japan* *Bull. Chem. Soc. Jpn.*, **71**, *883—891 (1998)*

Effect of a Sterically Hindered Imidazole Ligand on the Molecular Structure and Axial Ligand Substitution Reaction of the Chromium(III) Porphyrin Complex

Masahiko Inamo* **and Kiyohiko Nakajima**

Department of Chemistry, Aichi University of Education, Hirosawa 1, Igaya, Kariya 448-8542

(Received November 17, 1997)

A structural, thermodynamic, and kinetic study of a chromium(III) complex of 5,10,15,20-tetraphenylporphyrin, [Cr(tpp)(Cl)(L)], where L represents an imidazole ligand, is presented. The present study is aimed at elucidating the effect of a steric strain induced by the 2-methyl substituent of the imidazole ligand on the molecular structure and the dynamics of an axial ligand-substitution reaction. Crystals of the 1-methylimidazole complex [Cr(tpp)(Cl)(1-Meim)] (**1**) and 1,2-dimethylimidazole complex [Cr(tpp)(Cl)(1,2-Me_2im)] (**2**) were obtained from a dichloroethane–toluene mixture containing a slight excess of imidazole ligand in the monoclinic space group *Cc*, $Z=4$, $a=18.306(2)$, $b=13.311(2)$, $c=21.391(5)$ Å, $\beta=120.05(1)^\circ$, $V=4512(1)$ Å^3, and in the orthorhombic space group $P2_12_12_1$, $Z=4$, $a=9.926(1)$, $b=17.902(3)$, $c=25.247(4)$ Å, $V=4486(1)$ Å^3, respectively. The axial Cr–N_{im} bond lengths for **1** and **2** are 2.103(4) and 2.139(5) Å, respectively. A steric hindrance has been demonstrated by a 0.036 Å increase in the Cr–N_{im} bond length and a tilting and tipping of the imidazole ligand of **2** from the symmetrical position observed in **1**. The substitution reaction of the axial pyridine ligand of [Cr(tpp)(Cl)(py)] by various imidazole ligands was studied spectrophotometrically in dichloromethane or in toluene. A steric effect due to the 2-methyl substituent of the imidazole ligand was observed along with an increase in the ligand-dissociation rate and a decrease in the binding constant of the imidazole ligand to the metalloporphyrin. These results were examined in terms of steric interactions between the axial ligand and the porphyrin core.

Metalloporphyrins are important model compounds for understanding the biological functions of heme proteins. One of the characteristic features of metalloporphyrins caused by the porphyrin ligation is an acceleration of the axial ligand-substitution reaction, which is closely related to the biological functions, such as oxygen transport and storage by heme proteins. Such a labilization effect amounts to several orders of magnitude or more in rate, especially for those of chromium(III),[1)] cobalt(III),[2)] and rhodium(III)[3] ions, which are usually substitution inert. Kinetic studies on the axial-substitution reaction of metalloporphyrins have been extensively carried out in order to elucidate the mechanism of the labilization effect. The reaction mechanism was evidenced or proposed on the basis of the rate law, activation parameters, and the substituent effect of the reaction, and the axial substitution reaction has been proved to proceed via a dissociative or dissociative-interchange mechanism for many metalloporphyrins. As for chromium(III) porphyrins, the mechanism of the axial substitution reaction has been suggested to be a limiting dissociative mechanism, and a coordinately unsaturated complex was assumed as a reaction intermediate.[1f,11)] In such a case, laser photolysis can sometimes be successfully employed to elucidate the properties of the intermediate generated by the photodissociation of the axial ligand, providing direct evidence for the reaction mechanism.[4)]

In an attempt to obtain further information about the reaction mechanism, it is worth investigating the substitution reaction from the viewpoint of the steric effect, because it is expected that such an approach will provide further insight into the relationship between the molecular structure and the reactivity of the molecule. The steric effect of the bulky substituent of the axial ligand on the properties of metalloporphyrins has been mainly discussed based on the molecular structure of metalloporphyrins, and very few examples are known for the dynamics of the axial substitution reaction.[5)] The aims of this paper are (i) to establish the molecular structure of chromium(III) porphyrin complexes and (ii) to clarify the relation between the molecular structure and the steric effect on the chemical reactivity of metalloporphyrins. We report here on the structure of chromium(III) porphyrins which have five-membered imidazoles as an axial ligand and the equilibria and kinetics of their ligand substitution reactions in an organic solvent.

Experimental

Reagents. Chloro(5, 10, 15, 20- tetraphenylporphinato)-chromium(III) [Cr(tpp)(Cl)] was prepared and purified according to the reported procedure.[6)] Pyridine (py, Wako Pure Chemicals, Japan) and 1-methylimidazole (1-Meim, Aldrich) were dried with solid NaOH and then distilled. 1,2-Dimethylimidazole (1,2-Me_2im, Aldrich), 5-chloro-1-methylimidazole (5-Cl-1-Meim, Aldrich), and 1-acetylimidazole (1-Acim, Aldrich) were used without further purification. Toluene was washed with concentrated sulfuric acid and water and then distilled over sodium. Dichloromethane dried over 3-Å molecular sieves was distilled; then, a small amount of 2-methyl-2-butene (Aldrich) was added as a stabilizer. Crystals of [Cr(tpp)(Cl)(1-Meim)] (**1**) were obtained by the following procedure. Sixty mg of [Cr(tpp)(Cl)] and 50 mg of 1-Meim were dissolved in 4 cm^3 of hot 1,2-dichloroethane and 20 cm^3 of hot toluene was added to the solution. After the mixture was filtered, the filtrate was set aside in the dark for several days, allowing a slow evaporation of the solvent. The precipitated purple crystalline product was collected via filtration and dried in vacuum at room temperature for several hours. Anal. Calcd for [Cr(tpp)(Cl)-(1-Meim)]·(1/4)$C_2H_4Cl_2$: C, 72.18; H, 4.37; N, 10.41%. Found: C, 72.02; H, 4.53; N, 10.30%. Crystals of [Cr(tpp)(Cl)(1,2-Me_2im)] (**2**) were prepared by a procedure similar to that described above. Anal. Calcd for [Cr(tpp)(Cl)(1,2-Me_2im)]·(2/3)$C_2H_4Cl_2$: C, 70.11; H, 4.52; N, 9.75%. Found: C, 70.38; H, 4.23; N, 9.43%.

Measurements. UV-visible absorption spectra were recorded on a Hitachi U-3000 spectrophotometer. Kinetic measurements were performed with a stopped-flow spectrophotometer (Unisoku, Japan). The temperature of the reaction solutions was controlled to within ±0.1 °C using a circulating thermostatted water bath. The concentrations of the leaving and entering ligands were kept in large excess over that of the chromium(III) porphyrin complex to guarantee the pseudo-first-order conditions. The total concentration of the complex was in the range of $(0.5—1.2)\times 10^{-5}$ mol kg^{-1}. The pseudo-first-order rate constnat (k_{obs}) was evaluated by fitting the absorbance-time traces with a non-linear least-squares program. The reporducibility of the k_{obs} value was better than ±5%. The concentration of water in the toluene or dichloromethane solution, which was determined by the Karl–Fischer titrator (CA-06, Mitsubishi Kasei, Japan), was kept as low as possible (usually less than 3×10^{-3} mol kg^{-1}).

X-Ray Structure Analysis. Single crystals (**1** or **2**) suitable for X-ray analysis were mounted on a glass fiber using epoxy resin. Unit cell constants of each complex were determined by a least-squares refinement of the angular positions of 25 accurately centered independent reflections. Intensity data were collected at ambient temperature on a Rigaku AFC7R (for **1**) and an Enraf–Nonius CAD4 (for **2**) diffractometer using graphite monochromatized Mo $K\alpha$ radiation ($\lambda = 0.71069$ Å) with an ω–2θ scan mode. Systematic extinctions and diffraction symmetry for the preliminary data suggested alternatively the monoclinic space group *Cc* (No. 9) or *C*2/*c* (No. 15) for **1** and unequivocally the orthorhombic $P2_12_12_1$ (No. 19) for **2**. The noncentrosymmetric space group *Cc* chosen for **1** was later proved to be correct by a successful solution and refinement of the model. Crystallographic data and experimental details are listed in Table 1. Three standard reflections were monitored at every 150 reflections for **1** and an interval of 2 h for **2** throughout the data collection, and no significant deterioration was observed. Absorption corrections were applied on the basis of ψ scans for **1**. The position of the chromium was determined by direct methods (SHELXS 86)[7] for each complex, and the remaining non-hydrogen atoms were located by subsequent Fourier syntheses. The structure was refined on *F* by full-matrix least-squares techniques with anisotropic thermal parameters for non-hydrogen atoms. All of the hydrogen atoms were placed at calculated positions with the isotropic displacement parameters of the carbon atoms to which they were attached, but were not included in least-squares refinement. The solvent dichloroethane molecules in **1** and **2** were badly resolved. The positions and displacement parameters of the heavily disordered atoms of dichloroethane molecules were fixed for the final cycles of refinement. For **2**, the Cl atoms of the dichloroethane molecule were disordered over two sites with an occupancy ratio of 1/1. The calculations were carried out with the Xtal 3.2[8] software. The structures of **1** and **2** are noncentrosymmetric, and the presented structures are significant at the 0.005 level when Hamilton's *R* factor test[9] is applied. The atomic coordinates, thermal parameters, bond distances and angles, and $F_o - F_c$ tables were deposited as Document No. 71020 at the Office of the Editor of Bull. Chem. Soc. Jpn.

Table 1. Summary of Crystal Structure Data

	[Cr(tpp)(Cl)(1-Meim)]·(1/4)$C_2H_4Cl_2$	[Cr(tpp)(Cl)(1,2-Me_2im)]·(2/3)$C_2H_4Cl_2$
Formula	$C_{48.5}H_{35}N_6Cl_{1.5}Cr$	$C_{50.33}H_{38.67}N_6Cl_{2.33}Cr$
FW	807.03	862.13
Crystal system	Monoclinic	Orthorhombic
Space group	*Cc* (No. 9)	$P2_12_12_1$ (No. 19)
Crystal dimensions/mm	$0.13\times 0.28\times 0.60$	$0.18\times 0.30\times 0.50$
a/Å	18.306(2)	9.926(1)
b/Å	13.311(2)	17.902(3)
c/Å	21.391(5)	25.247(4)
β/deg	120.05(1)	
Z	4	4
V/$Å^3$	4512(1)	4486(1)
μ(Mo $K\alpha$)/cm^{-1}	3.73	4.27
d_{calcd}/g cm^{-3}	1.19	1.28
T/K	298	298
$2\theta_{max}$/deg	60	60
No. of reflections measd	6748	7530
No. of reflections obsd [$\lvert F_o \rvert > 3\sigma(\lvert F_o \rvert)$]	4980	3965
No. of parameters refined	503	514
$R^{a)}$	0.060	0.059
${R_w}^{b)}$	0.080	0.062
$S^{c)}$	2.90	1.79

a) $R=\sum||F_o|-|F_c||/\sum|F_o|$. b) $R_w=[\sum w||F_o|-|F_c||^2/\sum w|F_o|^2]^{1/2}$, $w=[\sigma^2(F_o)+\{0.020(F_o)\}^2]^{-1}$ for **1** and $w=[\sigma^2(F_o)+\{0.015(F_o)\}^2]^{-1}$ for **2**. c) $S=[\sum w||F_o|-|F_c||^2/(m-n)]^{1/2}$ (m = no. of used reflections, n = no. of refined parameters).

Results and Discussion

Figure 1 shows the molecular structure of **1** with the atom labeling scheme used throughout this paper. The selected bond lengths and angles for **1** are listed in Table 2. Figure 2 shows the perpendicular displacements (in units of 0.01 Å) of the atoms from the mean plane of the respective 24-atom porphyrin core (P_{core}). The root-mean-square displacement from P_{core} for the entire core is 0.038 Å. The chromium atom is located 0.033 Å from P_{core} and 0.042 Å from the plane of four pyrrole nitrogens (P_N) toward the chloride. The four equatorial Cr–N lengths (2.057(7), 2.022(5), 2.004(7), and 2.042(5) Å) are close to each other. As can be seen from Fig. 2, the axial imidazole plane is slightly tilted from the normal to the mean skeletal plane of the porphyrin. The dihedral angle between the imidazole plane and the 24-atom core for the porphyrin is 78.8(2)°. Such derivations have been commonly noted for imidazole derivatives coordinated to metalloporphyrins.[10] The dihedral angle (ϕ) between the imidazole plane and the plane defined by [N(1), Cr, N(3), N(5)] is 17.3(3)°. The dihedral angles between the peripheral phenyl groups and the mean plane of the 24-atom core are within the normal range with values of 78.0(3)°, 80.5(3)°,

Table 2. Selected Bond Lengths (Å) and Bond Angles (deg) for **1**

	Bond lengths		
Cr–Cl(1)	2.317(2)	Cr–N(1)	2.057(7)
Cr–N(2)	2.022(5)	Cr–N(3)	2.004(7)
Cr–N(4)	2.042(5)	Cr–N(5)	2.103(4)
N(5)–C(45)	1.36(1)	N(5)–C(47)	1.320(9)
N(6)–C(46)	1.36(1)	N(6)–C(47)	1.326(8)
N(6)–C(48)	1.47(1)	C(45)–C(46)	1.345(9)
	Bond angles		
Cl(1)–Cr–N(1)	90.3(1)	Cl(1)–Cr–N(2)	91.2(1)
Cl(1)–Cr–N(3)	91.9(1)	Cl(1)–Cr–N(4)	91.3(1)
Cl(1)–Cr–N(5)	177.3(2)	N(1)–Cr–N(2)	89.0(3)
N(1)–Cr–N(3)	177.7(2)	N(1)–Cr–N(4)	88.7(2)
N(1)–Cr–N(5)	90.1(2)	N(2)–Cr–N(3)	91.7(3)
N(2)–Cr–N(4)	176.6(2)	N(2)–Cr–N(5)	86.1(2)
N(3)–Cr–N(4)	90.5(2)	N(3)–Cr–N(5)	87.8(2)
N(4)–Cr–N(5)	91.4(2)	Cr–N(5)–C(45)	127.1(5)
Cr–N(5)–C(47)	127.1(5)	C(45)–N(5)–C(47)	105.0(5)
N(5)–C(45)–C(46)	109.1(8)	N(6)–C(46)–C(45)	107.4(7)
C(46)–N(6)–C(47)	106.2(6)	N(5)–C(47)–N(6)	112.3(7)
C(46)–N(6)–C(48)	126.8(6)	C(47)–N(6)–C(48)	126.9(7)

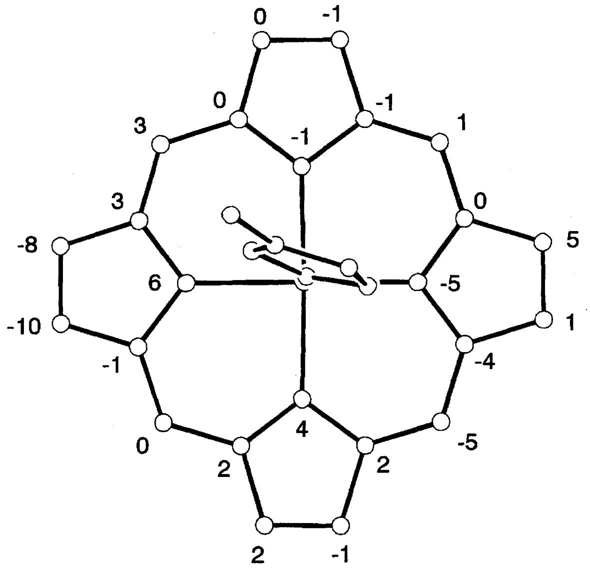

Fig. 2. Diagram of the 24-atom porphyrin core in [Cr(tpp)(Cl)(1-Meim)] (**1**) showing displacements (in units of 0.01 Å) of each atom from the mean plane of the core. Positive values indicate a displacement on the imidazole side of the plane.

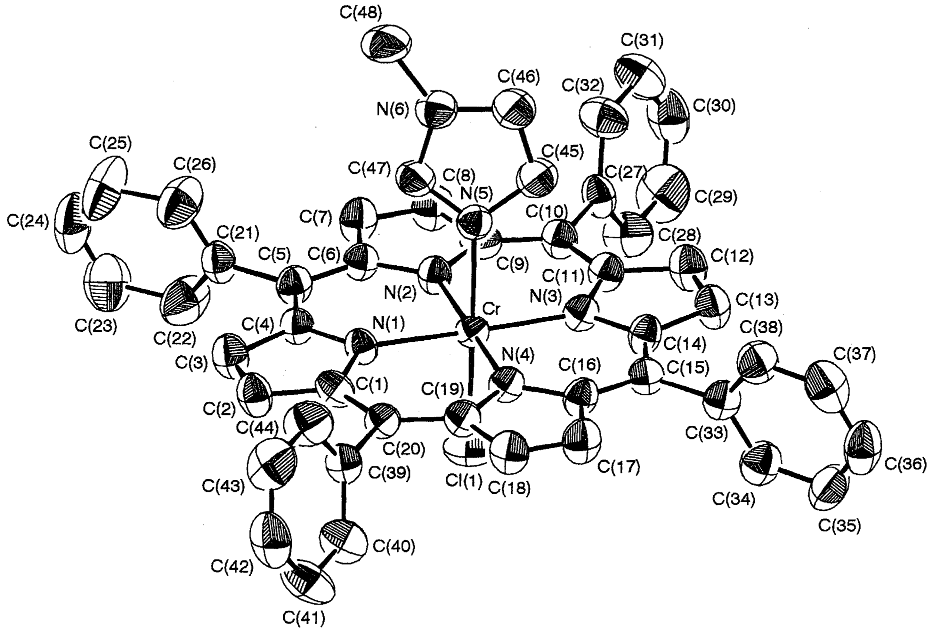

Fig. 1. Molecular structure of [Cr(tpp)(Cl)(1-Meim)] (**1**).

79.5(2)°, and 74.6(3)°.

Figures 3 and 4 and Table 3 give the relevant structural features for **2**. As is commonly seen with six-coordinate metalloporphyrins,[11] the porphyrin core displays approximate S_4 ruffling with the methine carbons alternating above and below the mean plane of the 24-atom core with an average absolute displacement of 0.061 Å. The rms displacement for the entire core is 0.137 Å. The chromium atom projects slightly toward the imidazole ligand, being 0.052 and 0.011 Å from P_{core} and P_N, respectively. The Cr–N_{im} bond length of **2** is longer by 0.036 Å than **1**. The imidazole plane is almost perpendicular to the porphyrin plane in **2**. The dihedral angle between the porphyrin core and the imidazole plane is 88.1(2)°. The dihedral angle (ϕ) between the imidazole plane and the plane defined by [N(1), Cr, N(3), N(5)] is 41.5(3)°. The axial Cr–N(5) bond is tilted by ca. 4° from the porphyrin normal. The unequal Cr–N(5)–C(45) (120.0(4)°) and Cr–N(5)–C(47) (134.4(4)°) angles are due to the nonbonded interaction between the imidazole 2-methyl group and the porphyrin core, resulting in the tipping of the imidazole ligand of ca. 7°. The dihedral angles between the

Table 3. Selected Bond Lengths (Å) and Bond Angles (deg) for **2**

	Bond lengths		
Cr–Cl(1)	2.315(2)	Cr–N(1)	2.058(4)
Cr–N(2)	2.024(5)	Cr–N(3)	2.034(4)
Cr–N(4)	2.029(4)	Cr–N(5)	2.139(5)
N(5)–C(45)	1.381(9)	N(5)–C(47)	1.323(8)
N(6)–C(46)	1.36(1)	N(6)–C(47)	1.347(9)
N(6)–C(48)	1.49(1)	C(45)–C(46)	1.34(1)
C(47)–C(49)	1.50(1)		
	Bond angles		
Cl(1)–Cr–N(1)	89.8(1)	Cl(1)–Cr–N(2)	91.0(1)
Cl(1)–Cr–N(3)	88.3(1)	Cl(1)–Cr–N(4)	89.8(1)
Cl(1)–Cr–N(5)	175.5(2)	N(1)–Cr–N(2)	89.8(2)
N(1)–Cr–N(3)	178.2(2)	N(1)–Cr–N(4)	90.6(2)
N(1)–Cr–N(5)	93.2(2)	N(2)–Cr–N(3)	90.1(2)
N(2)–Cr–N(4)	179.2(2)	N(2)–Cr–N(5)	92.4(2)
N(3)–Cr–N(4)	89.4(2)	N(3)–Cr–N(5)	88.6(2)
N(4)–Cr–N(5)	86.9(2)	Cr–N(5)–C(45)	120.0(4)
Cr–N(5)–C(47)	134.4(4)	C(45)–N(5)–C(47)	105.5(5)
C(46)–N(6)–C(47)	106.9(6)	C(46)–N(6)–C(48)	124.1(6)
C(47)–N(6)–C(48)	128.9(6)	N(5)–C(45)–C(46)	109.1(7)
N(6)–C(46)–C(45)	107.6(7)	N(5)–C(47)–N(6)	110.9(6)
N(5)–C(47)–C(49)	127.0(6)	N(6)–C(47)–C(49)	122.1(6)

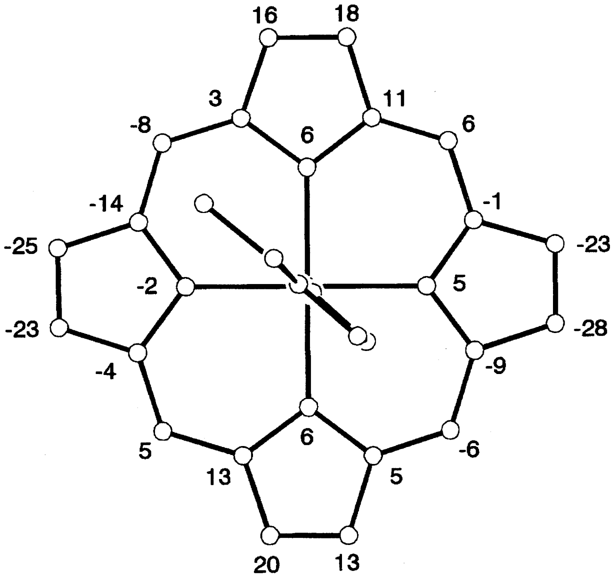

Fig. 4. Diagram of the 24-atom porphyrin core in [Cr(tpp)(Cl)(1,2-Me_2im)] (**2**) showing displacements (in units of 0.01 Å) of each atom from the mean plane of the core. Positive values indicate a displacement on the imidazole side of the plane.

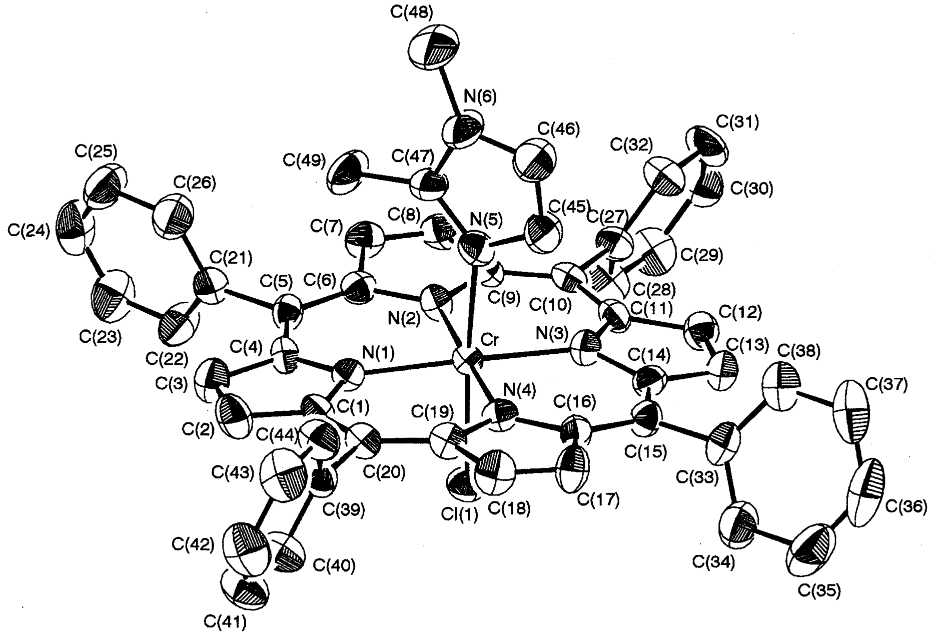

Fig. 3. Molecular structure of [Cr(tpp)(Cl)(1,2-Me_2im)] (**2**).

peripheral phenyl groups and the mean plane of the 24-atom core are within the normal range with values of 76.9(2)°, 67.4(2)°, 61.9(2)°, and 74.7(2)°.

It is expected that introducing the sterically demanding 2-methyl substituent onto the axial imidazole ligand causes the intramolecular steric interactions between the methyl group and the porphyrin core. We have summarized the structural parameters of several imidazole complexes in Table 4. In the present case, there are substantial differences between the structures of **1** and **2**, which can be ascribed to the 2-methyl substituent. While the Cr–Cl and Cr–N_P bond lengths are not influenced by the presence of the 2-methyl group, the bond length between Cr and the imidazole nitrogen atom of **2** is longer than that of **1**. The difference in the Cr–N_{im} bond length of 0.036 Å is, however, smaller than that observed in [Fe(tpp)(N_3)(L)]. This can be ascribed to the shorter M–N_{im} bond length of the Fe(III) porphyrin complexes than the corresponding bond lengths of the chromium(III) porphyrins. These steric interactions cause pronounced S_4 ruffling of the porphyrin core in order to avoid unfavorable interactions between the 2-methyl group and the porphyrin core in **2**. Such interactions are also well reflected in the orientation of the axial imidazole ligand in metalloporphyrin complexes. A convenient measure of the orientation of the axial planar ligand is the dihedral angle (ϕ) between the imidazole plane and a place containing opposing nitrogen atoms of the porphyrin core and coordinated axial atom(s).[21)] A value of 0° for ϕ corresponds to an eclipsed conformation and a value of 45° to a staggered conformation. The value of ϕ for **1** is 17°, almost eclipsing the equatorial Cr–N_P bonds. This value is smaller than would be expected on simple steric grounds. This situation is often met with the metalloporphyrin complexes having axial imidazole derivatives.[11)] The theoretical explanation of this tendency towards a small value of ϕ in the imidazole complex was thought to be due to the M–N_{im} π-bond, which favors eclipsed conformations.[22)] Another important structural feature imposed by the 2-methyl group is the tilting and tipping of the imidazole ligand. While there seems to be no appreciable tilting or tipping of the imidazole ligand for complex **1**, a tilting of 4° and a tipping of 7° in complex **2** indicate the presence of unfavorable nonbonded interactions between the axial ligand and the porphyrin core. Such tipping has also been reported for Fe(III) porphyrins,[12,14,16,18)] Co(II) porphyrins,[20)] and [Fe(TpivPP)(L)(O_2)][23)] when steric interactions due to the 2-methyl substituent of the axial imidazole ligand are introduced in the complex. The effects of the 2-methyl substituent on the molecular structure are summarized as (i) an increase in the ϕ value, (ii) greater ruffling of the porphyrin core, (iii) lengthening of the M–N_{im} bond length, and (iv) a tilting and/or tipping of the imidazole ligand.

We previously reported a structural characterization of [Cr(tpp)(Cl)(py)].[4c)] Although the average Cr–N_P bond length of 2.026(11) Å of the pyridine complex is close to that of **1**, the Cr–N_{py} bond length (2.140(5) Å) is 0.037 Å longer than the Cr–N_{im} bond length of **1**, which is occasionally almost the same as that of **2**. The value of the dihedral angle (ϕ (41°)) and the degree of the porphyrin core ruffling for [Cr(tpp)(Cl)(py)] are greater than **1**. Any resemblance in the structural features between [Cr(tpp)(Cl)(py)] and **2**, rather than **1**, can be reasonably explained by the steric effect, because it is expected that the six-membered pyridine ring experiences greater steric hindrance at the axial site of the metalloporphyrins than the five-membered imidazole ring due to the greater intramolecular nonbonded interactions between the pyridine α-hydrogen atoms and the porphyrin core.

It is well-known that the axial substitution reaction of ligand L of the chromium(III) porphyrin complex by the entering ligand X occurs relatively fast in non-coordinating organic solvents according to Eq. 1.[1f,11,6)] In order to examine the steric effect of the bulky substituent of the imidazole

Table 4. Summary of M–N Bond Distances, Relative Orientation of Imidazole Ligands, and Core Conformation in Metalloporphyrins

Compound	M–N_P[a)]	M–N_L[b)]	ΔM–N_L[c)]	α[d,e)]	β[d,e)]	ϕ[e,f)]	C[g)]	Ref.
[Cr(tpp)(Cl)(1-Meim)]	2.031(7)	2.103(4)		127.1(5)	127.1(5)	17.3(3)	10	This work
[Cr(tpp)(Cl)(1,2-Me_2im)]	2.036(5)	2.139(5)	0.036	134.4(4)	120.0(4)	41.5(3)	28	This work
[Fe(tpp)(N_3)(1-Meim)]	1.988(5)	1.987(5)		126.8(4)	128.9(5)	38.3	40	12
[Fe(tpp)(N_3)(1,2-Me_2im)]	1.983(8)	2.070(8)	0.083	133.8(8)	119.1(8)	43.4	43	12
[Fe(oep)$(Him)_2$]$^+$						7		13
[Fe(oep)$(2\text{-}MeHim)_2$]$^+$	2.041(1)	2.275(1)		134.15(10)	120.76(9)	22	7	14
[Fe(tpp)$(Him)_2$]$^+$	1.994(3)	1.977(3)		127.3(3)	127.8(3)	5.7	4	15
	1.993(3)	1.964(3)		125.7(3)	128.8(3)	41.4	7	15
[Fe(tpp)$(2\text{-}MeHim)_2$]$^+$	1.971(4)	2.013(4)	0.042	132.9(4)	120.6(4)	32	41	16
[Fe(tmp)$(1\text{-}Meim)_2$]$^+$	1.988(20)	1.975(3)		127.0(2)	128.7(3)	23	4	17
	1.987(1)	1.965(3)		128.3(3)	129.4(3)	41	9	17
[Fe(tmp)$(1,2\text{-}Me_2im)_2$]$^+$	1.937(5)	2.004(5)	0.034	134.6(5)	119.8(4)	44.9	75	18
[Co(tpp)(1-Meim)]	1.977(3)	2.157(3)		127.8(3)	126.4(3)	0	13	19
[Co(tpp)(1,2-Me_2im)]	1.985(2)	2.216(2)	0.059	132.6(2)	122.5(2)	20	14	20

a) M–N_P is the average bond length (Å) between the central metal ion and the porphyrin nitrogen atoms. b) M–N_L is the bond length (Å) between the central metal ion and the nitrogen atom of the axial imidazole ligand. c) ΔM–N_L is the difference in M–N_L value (Å) between the complex having 2-methyl group in its axial imidazole ligand and that having no 2-methyl group. d) α and β represent pairs of M–N_{im}–C_{im} angles. e) Value in degrees. f) See in text. g) Maximum absolute displacement of any core atom from the 24-atom core plane. Values in units of 0.01 Å.

ligand on equilibria and kinetics of the axial substitution reaction, we have investigated reaction 1 by the spectrophotometric method. In the present study, pyridine was used as

$$[\mathrm{Cr(tpp)(Cl)(L)}] + \mathrm{X} \rightleftharpoons [\mathrm{Cr(tpp)(Cl)(X)}] + \mathrm{L} \qquad (1)$$

a leaving ligand L and 1-Meim, 5-Cl-1-Meim, 1-Acim, or 1,2-Me_2im were used as an entering ligand X. Dichloromethane or toluene was used as a solvent. The equilibrium constant (K) for reaction 1 was determined by a conventional spectrophotometric method. The visible absorption spectra of the chromium(III) porphyrin complexes are shown in Fig. S1 which is deposited as Document No. 71020 at the Office of the Editor of Bull. Chem. Soc. Jpn. The spectrophotometric titration of a [Cr(tpp)(Cl)(py)] solution with substituted imidazole was conducted in the presence of pyridine in large excess over the complex. In dichloromethane, for example, the initial pyridine complex with a Soret band at 457 nm was converted with good isosbestic points into a species with a higher Soret band in the range of 453—457 nm. The progress of the reaction was monitored by observing the absorbance changes at several wavelengths of the visible spectra as a function of the concentrations of leaving and entering ligands. The equilibrium constants were determined by simultaneously analyzing the absorbance data at several wavelengths between 350 and 500 nm from a least-squares fit of the data. An analysis of the data confirmed the stoichiometry indicated in Eq. 1. A quantitative determination of the equilibrium constant (K) was carried out in at least two experiments for each imidazole ligand in the temperature range between 15 and 35 °C. The thermodynamic constants ΔH° and ΔS° were determined by van't Hoff plots of $\ln K$ vs. $1/T$ (K). The values of the equilibrium constant and thermodynamic parameters are listed in Table 5.

The rate constants of the substitution reaction of py on [Cr(tpp)(Cl)(py)] by the entering ligand X (reaction 1) were determined by a stopped-flow method. The rates of the reaction were measured under various conditions where entering and leaving ligands were present in large excess over the porphyrin complex. The reaction was first order with respect to the porphyrin complex. The pseudo-first-order rate constant (k_{obs}) is plotted against the ratio of the concentration of entering and leaving ligands in the bulk solution in Fig. 5 for X=1,2-Me_2im. At a constant concentration of pyridine in the bulk, the rate constants increase with an increase in [1,2-Me_2im], but level off at a higher 1,2-Me_2im concentration, while the rates decrease along with an increase in the concentration of pyridine in the bulk at a constant 1,2-Me_2im concentration. These features can be interpreted by a dissociative mechanism indicated by Eqs. 2 and 3. A steady-state approximation to the five-coordinate intermediate [Cr(tpp)(Cl)] gives Eq. 4. The values of k_1, $k_2k_3^{-1}$, and k_4 at

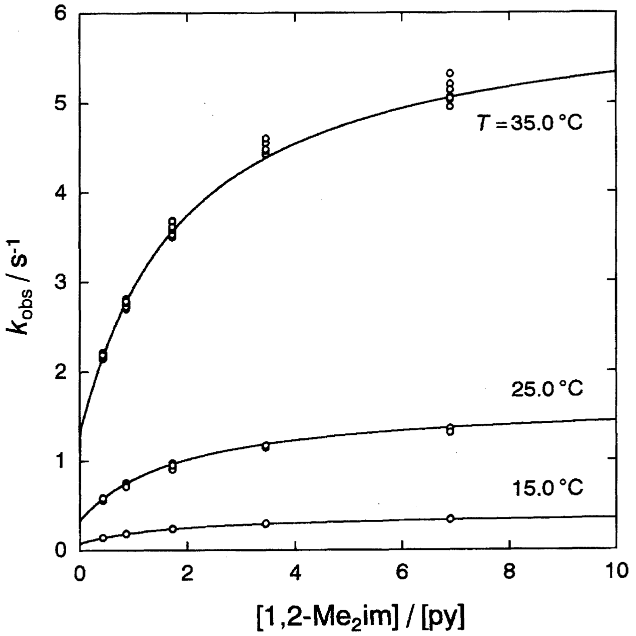

Fig. 5. Dependence of the first-order rate constant k_{obs} on the ratio of [1,2-Me_2im]/[py] at various temperatures. The concentration of the chromium(III) porphyrin complex is $(0.5—1.2)\times10^{-5}$ mol kg^{-1}. Total concentration of 1,2-Me_2im and py is in the range of 1×10^{-3}—4×10^{-2} mol kg^{-1}. The solid curves were calculated by using the activation parameters obtained.

Table 5. Equilibrium Constants and Thermodynamic Parameters for Substitution Reaction of the Axial Pyridine Ligand of [Cr(tpp)(Cl)(py)] by the Entering Ligand X[a)]

Solvent	X	pK_a[b)]	K (25.0 °C)	ΔH° / kJ mol^{-1}	ΔS° / J K^{-1} mol^{-1}
CH_2Cl_2	1-Meim	7.2[c)]	$(2.35\pm0.08)\times10^2$	-14.4 ± 0.5	-2.9 ± 1.7
	5-Cl-1-Meim	5.1[d)]	$(2.53\pm0.12)\times10$	-8.7 ± 0.3	-2.4 ± 1.1
	1-Acim	3.6[e)]	6.0 ± 0.4[f)]	-6.0 ± 7.8[f)]	-5 ± 26[f)]
	1,2-Me_2im	8.2[g)]	2.68 ± 0.10	-6.9 ± 0.3	-14.9 ± 1.0
Toluene	1-Meim	7.2[e)]	$(3.31\pm0.04)\times10^2$	-14.6 ± 0.4	-0.7 ± 1.4
	1,2-Me_2im	8.2[g)]	4.87 ± 0.21	-3.4 ± 0.8	1.7 ± 2.7

a) Errors represent the standard deviation. b) pK_a of the conjugate acid of X. c) Ref. 24. d) Ref. 25. e) Ref. 26. f) Thermodynamic constants for 1-Acim reaction were estimated by using kinetic parameters, because a slow side reaction which causes a slight change in absorption spectra occurs for this reaction system. g) Ref. 27.

$$[\mathrm{Cr(tpp)(Cl)(L)}] \underset{k_2}{\overset{k_1}{\rightleftharpoons}} [\mathrm{Cr(tpp)(Cl)}] + \mathrm{L} \quad (2)$$

$$[\mathrm{Cr(tpp)(Cl)}] + \mathrm{X} \underset{k_4}{\overset{k_3}{\rightleftharpoons}} [\mathrm{Cr(tpp)(Cl)(X)}] \quad (3)$$

$$k_{\mathrm{obs}} = (k_1\,[\mathrm{X}] + k_4(k_2k_3{}^{-1})\,[\mathrm{py}])((k_2k_3{}^{-1})\,[\mathrm{py}] + [\mathrm{X}])^{-1} \quad (4)$$

each temperature were determined by fitting k_{obs} obtained at various concentrations of pyridine and X to Eq. 4 using a least-squares programs. In some cases, k_4 is too small to be determined from the kinetic results, especially for X= 1-Meim. k_4 in Eq. 4 was then substituted with $k_1k_3k_2{}^{-1}K^{-1}$, and kinetic results were analyzed with K values obtained independently by a spectrophotometric titration to determine k_1 and $k_2k_3{}^{-1}$. Eyring's plots of k_1, $k_2k_3{}^{-1}$, and k_4 proved linear within experimental error for all reactions. Therefore, the enthalpy and entropy of activation were determined by simultaneously fitting the variable-temperature data to Eq. 4 and the Eyring equation. The values of the rate constants and kinetic parameters are summarized in Tables 6 and 7, respectively.

General conclusions that may be drawn from the data presented above are best appreciated by an examination of Fig. 6. The equilibrium constant and rate constants are related to the basicity of the free ligand, here the pK_a value of the conjugate acid of the ligand. We first consider the equilibria of the reaction. For a series of imidazole ligands there is a correlation between the value of log K and pK_a among the nonhindered ligands, although a limited number of ligands were employed. The well-known relationship[28] is therefore obeyed by the nonhindered imidazoles: log K=0.46 pK_a−0.96. We have previously studied the equilibria and kinetics of the axial substitution reaction of [Cr(tpp)(Cl)(L)] by 1-Meim, where L represents substituted pyridines which have substituents at their β- and/or γ-positions, and the linear free-energy relationship between equilibrium constants (or rate constants) and the basicity of the pyridine ligands was found.[11] These results are also included in Fig. 6. For substituted pyridines, the results yield a reasonably linear relationship between log K vs. pK_a: log K=−0.36 pK_a+2.71. A similar relationship was observed for the Co(II) porphyrin in toluene[29] and Fe(II) porphyrin microperoxidase-8 in aqueous methanol.[25,30] The trend observed for these reactions is that the higher is the basicity of the ligand the higher is the binding constant, which can be easily understood from the viewpoint of the electronic effect of the substituents.

The effect of a bulky substituent bound to the α-carbon atom adjacent to the coordinating nitrogen atom of imidazole is clearly seen in Fig. 6. The value of log K=0.43 for 1,2-Me$_2$im indicates that the steric hindrance has suppressed log K by 2.4 below the "baseline" of the linear free-energy relationship for the nonhindered imidazoles in dichloromethane. Usually, imidazole ligands having a five-membered ring tend to bind more tightly to metalloporphyrins than do six-membered pyridines. In the present case, the steric effect due to the bulky substituent occasionally lowers the binding constant of 1,2-Me$_2$im to that comparable to the pyridine complex. This is in accord with the structural feature of these molecules, where the axial Cr–N$_{\mathrm{L}}$ bond lengths for [Cr(tpp)(Cl)(py)] and **2** are close to each other and longer than that for **1**. A similar steric effect was observed for

Table 6. Rate Constants for the Substitution Reaction of Pyridine of [Cr(tpp)(Cl)(py)] by X[a)]

Solvent	X	k_1/s^{-1} (25.0 °C)	$k_2k_3{}^{-1}$ (25.0 °C)	k_4/s^{-1} (25.0 °C)
CH$_2$Cl$_2$	1-Meim	1.66±0.05[b)]	1.68±0.04	4.13×10^{-3} [c)]
	5-Cl-1-Meim		1.63±0.04	4.10×10^{-2} [c)]
	1-Acim		1.43±0.11	$(1.94\pm0.23)\times10^{-1}$
	1,2-Me$_2$im		1.85±0.14	$(3.32\pm0.13)\times10^{-1}$
Toluene	1-Meim[d)]	8.8±0.5[d)]	0.93±0.02	2.68×10^{-2}
	1,2-Me$_2$im		1.22±0.09	1.58±0.24

a) Errors represent the standard deviation. b) Average values calculated from those obtained for each reaction system. c) Calculated by using values of k_1, $k_2k_3{}^{-1}$, and K. d) Date are taken from Ref. 11.

Table 7. Kinetic Parameters for the Substitution Reaction of Pyridine of [Cr(tpp)(Cl)(py)] by the Entering Ligand X[a)]

Solvent	X	$\Delta H_1^{\ddagger}$	$\Delta S_1^{\ddagger}$	$\Delta H_2^{\ddagger}-\Delta H_3^{\ddagger}$	$\Delta S_2^{\ddagger}-\Delta S_3^{\ddagger}$	$\Delta H_4^{\ddagger}$	$\Delta S_4^{\ddagger}$
		kJ mol^{-1}	J K^{-1} mol^{-1}	kJ mol^{-1}	J K^{-1} mol^{-1}	kJ mol^{-1}	J K^{-1} mol^{-1}
CH$_2$Cl$_2$	1-Meim	97.2±1.4[b)]	85.1±4.5[b)]	2.3±1.2	12.0±3.9	109.8±1.3	77.7±4.3
	5-Cl-1-Meim			3.8±1.1	16.9±3.6	104.0±1.2	77.3±4.2
	1-Acim			−0.7±3.9	1±13	100.4±6.7	78±22
	1,2-Me$_2$im			3.8±3.6	18±12	101.2±2.2	85.2±7.5
Toluene	1-Meim	86.9±0.9[b)]	64.4±3.1[b)]	−1.6±1.0	−6.1±3.3	101.7±1.9	65.9±6.4
	1,2-Me$_2$im			−0.7±2.0	−0.7±5.4	91.8±2.0	66.9±6.6

a) Errors represent the standard deviation. b) Averaged values calculated from those obtained for each reaction system.

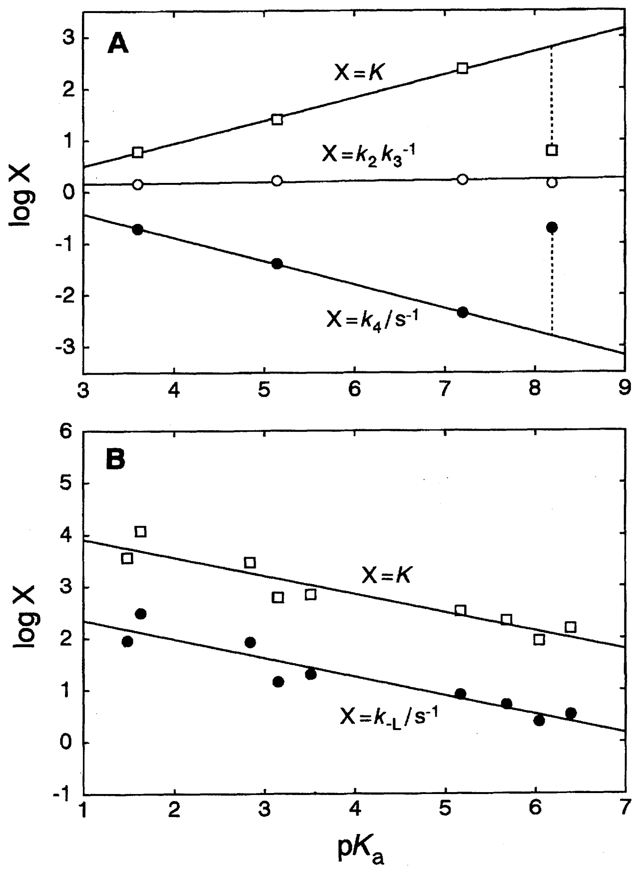

Fig. 6. Relationship between equilibrium constant K, rate constant k_4, or the ratio of rate constants $k_2k_3^{-1}$ at 25.0 °C in dichloromethane and the pK_a of the conjugate acid of the entering imidazole ligand X for the substitution reaction of py in [Cr(tpp)(Cl)(py)] by X in dichloromethane (A). Plots of $\log K$ vs. pK_a and $\log k_{-L}$ vs. pK_a for the substitution reaction of L in [Cr(tpp)(Cl)(L)] by 1-Meim at 25.0 °C in toluene (B), where pK_a is of the conjugate acid of various substituted pyridines (L) and k_{-L} represents the rate constant for the dissociation of L from [Cr(tpp)(Cl)(L)]. Data are taken from Ref. 11.

Co(II)–TPP[29] and Fe(III)–TPP[31] complexes. In the case of Co(II) porphyrins, a five-coordinate complex is produced through the reaction of a four-coordinate porphyrin complex with an entering ligand, and the binding constant for 1,2-Me$_2$im is smaller than that for 1-Meim by a factor of 4, while in the case of Fe(III) porphyrins, imidazole binding occurs in two steps, i.e., the first and second reactions give [Fe(tpp)(Cl)(L)] and [Fe(tpp)(L)$_2$]Cl, respectively, and the presence of the 2-methyl group of the imidazole ligand causes a decrease in the equilibrium constant of each reaction step by a factor of 3 and 60, respectively. For the present chromium(III) porphyrins, the decrease in the K value due to the 2-methyl group amounts to a factor of 88 and 68 in CH$_2$Cl$_2$ and toluene, respectively. Both for the Fe(III)–TPP and Cr(III)–TPP cases, a six-coordinate complex is formed, while the product is a five-coordinate complex in the Co(II)–TPP case. It is expected that the five-coordinate metalloporphyrin complexes suffer a smaller steric hindrance caused by the bulky groups adjacent to the aromatic nitrogen of the axial ligand than the six-coordinate metalloporphyrins, because the metal atom is displaced out of the porphyrin plane towards the axial ligand for the five-coordinate complex. Therefore, the weaker steric effect observed in the Co(II)–TPP case could be partly explained by these structural features of these complexes.

As in the case of the equilibria of the substitution reaction, the substituent effects on the kinetics of the axial substitution reaction are straightforward. As shown in Fig. 6, the rate constant for the dissociation of the imidazole ligand (k_4) is linearly correlated to the basicity of the ligand among nonhindered imidazoles. A similar correlation was previously observed for the dissociation of substituted pyridines from [Cr(tpp)(Cl)(L)] in toluene.[11] The slope of the straight lines in Fig. 6 is −0.47 and −0.36 for imidazoles and pyridines, respectively. The steric effect of the methyl group adjacent to the aromatic nitrogen of imidazole causes an acceleration of the off-rate of the ligand by a factor of ca. 200 with respect to the "baseline" of the linear free-energy relationship for the nonhindered imidazoles. The fact that the 1,2-Me$_2$im ligand dissociates much more easily than does 1-Meim is reflected by the difference in the molecular structure, especially the difference in the Cr–N$_{\mathrm{im}}$ bond length, which should be caused by the steric hindrance of the 2-methyl group in 1,2-Me$_2$im to the porphyrin core. The activation parameters also support these features. The trends observed in $\Delta H_4^{\ddagger}$ for the dissociation of imidazoles suggest that the electron-withdrawing group on the imidazole ring decreases the metal-ligand binding strength in these complexes for nonhindered imidazoles. The 2-methyl substituent causes a steric effect that decreases $\Delta H_4^{\ddagger}$ by about 10 kJ mol^{-1} from the "baseline" of the LFER. This decrease is the main factor controlling the acceleration of the off-rate of the ligand due to the steric effect.

On the contrary, the values of $k_2k_3^{-1}$ are independent of the substituents of the imidazoles, even for a sterically hindered imidazole. This indicates that the rate constant k_3 of binding of the imidazole ligand by the five-coordinate intermediate [Cr(tpp)(Cl)] shows no electronic or steric effects. These findings can be explained by the mechanism in which the rate-determining step of this ligand binding reaction may be the diffusion of two reacting molecules to make a precursor complex. Such a high reactivity of the intermediate [Cr(tpp)(Cl)] towards various nonhindered substituted pyridines has previously been discussed based on the substituent effects.[11] A small difference in the reactivity towards imidazole and pyridine ligands, which is demonstrated by the values of $k_2k_3^{-1}$, is also supporting evidence for the diffusion-controlled mechanism.

NMR studies on the Fe(III) and Co(III) porphyrin complexes have examined the axial bond weakening due to the steric effect of the 2-methyl group of imidazole ligands.[5] A comparison of the ligand dissociation rate between 1-Meim and 1,2-Me$_2$im reveals that the acceleration effect due to the 2-methyl substituent amounts to an increase by a factor of 920 for [Fe(tpp)(L)$_2$]Cl in CDCl$_3$ at 25 °C and 1400 for

$[Co(tpp)(L)_2]Cl$ in $CDCl_3$ at 90 °C. In the present case, k_4 for 1,2-Me_2im is 80-times that for 1-Meim at 25 °C in CH_2Cl_2. The acceleration effect for chromium(III) porphyrin is therefore much smaller than that for the bis-ligated complexes, such as $[Fe(tpp)(L)_2]Cl$ and $[Co(tpp)(L)_2]Cl$. These features are in accord with the degree of the S_4 ruffling of the porphyrin core. As can be seen in Table 4, the S_4 ruffling observed in the bis-ligated complex $[Fe(tpp)(L)_2]^+$ is greater than that of [Cr(tpp)(Cl)(L)]. The S_4 ruffling of the porphyrin core is a favorable solution to the steric demands involved in the formation of metalloporphyrins having hindered imidazoles. This means that the destabilization by some hindrance to the planarity of the porphyrin core due to the 2-methy group of the axial imidazole ligand is much more pronounced for the bis-ligated metalloporphyrins. An increased dissociation rate may be mainly caused by the fact that this strain will be released during the ligand-dissociation process, leading to a sterically less demanding five-coordinate intermediate. Therefore, a greater acceleration effect of the 2-methyl group on the ligand dissociation rate for Fe(III) porphyrin and Co(III) porphyrin complexes can be explained by the more extensive steric interactions between the axial ligand and the porphyrin core for these bis-ligated complexes than for the present chromium(III) porphyrin complexes.

References

1) E. B. Fleischer and M. Krishnamurthy, *J. Am. Chem. Soc.*, **93**, 3784 (1971); b) E. B. Fleischer and M. Krishnamurthy, *J. Coord. Chem.*, **2**, 89 (1972); c) M. Krishnamurthy, *Inorg. Chim. Acta*, **26**, 137 (1978); d) K. R. Ashley, J. G. Leipoldt, and V. K. Joshi, *Inorg. Chem.*, **19**, 1608 (1980); e) J. G. Leipoldt, S. S. Basson, and D. R. Rabie, *J. Inorg. Nucl. Chem.*, **43**, 3239 (1981); f) P. O'Brien and D. A. Sweigart, *Inorg. Chem.*, **21**, 2094 (1982); g) J. G. Leipoldt, R. van Eldik, and H. Kelm, *Inorg. Chem.*, **22**, 4146 (1983); h) J. G. Leipoldt and H. Meyer, *Polyhedron*, **6**, 1361 (1987); i) K. R. Ashley and J. Kuo, *Inorg. Chem.*, **27**, 3556 (1988); j) K. R. Ashley and I. Trent, *Inorg. Chim. Acta*, **163**, 159 (1989); k) M. Inamo, T. Sumi, N. Nakagawa, S. Funahashi, and M. Tanaka, *Inorg. Chem.*, **28**, 2688 (1989); l) M. Inamo, S. Sugiura, H. Fukuyama, and S. Funahashi, *Bull. Chem. Soc. Jpn.*, **67**, 1848 (1994).

2) a) E. B. Fleischer, S. Jacobs, and L. Mestichelli, *J. Am. Chem. Soc.*, **90**, 2527 (1968); b) R. F. Pasternack and M. A. Cobb, *Biochem. Biophys. Res. Commun.*, **51** 507 (1973); c) E. B. Fleischer and M. Krishnamurthy, *Ann. N. Y. Acad. Sci.*, **206**, 32 (1973); d) R. F. Pasternack and M. A. Cobb, *J. Inorg. Nucl. Chem.*, **35**, 4327 (1973); e) K. R. Ashley, M. Berggren, and M. Cheng, *J. Am. Chem. Soc.*, **97**, 1422 (1975); f) R. F. Pasternack, M. A. Cobb, and N. Sutin, *Inorg. Chem.*, **14**, 866 (1975); g) K. R. Ashley and S. Au-Young, *Inorg. Chem.*, **15**, 1937 (1976); h) R. F. Pasternack and G. R. Parr, *Inorg. Chem.*, **15**, 3087 (1976); i) K. R. Ashley, *J. Inorg. Nucl. Chem.*, **39**, 357 (1976); j) K. R. Ashley and J. G. Leipoldt, *Inorg. Chem.*, **20**, 2326 (1981); k) J. G. Leipoldt, S. S. Basson, G. J. Lamprecht, and R. D. Rabie, *Inorg. Chim. Acta*, **51**, 67 (1981); l) S. Funahashi, M. Inamo, K. Ishihara, and M. Tanaka, *Inorg. Chem.*, **21**, 447 (1982); m) A. Mahmood, H. Liu, J. G. Jones, J. O. Edwards, and D. A. Sweigart, *Inorg. Chem.*, **27**, 2149 (1988).

3) a) M. Krishnamurthy, *Inorg. Chim. Acta*, **25**, 215 (1977); b) K. R. Ashley, S. Shyu, and J. G. Leipoldt, *Inorg. Chem.*, **19**, 1613 (1980).

4) a) M. Yamaji, Y. Hama, and M. Hoshino, *Chem. Phys. Lett.*, **165**, 309 (1990); b) M. Yamaji, *Inorg. Chem.*, **30**, 2949 (1991); c) M. Inamo, M. Hoshino, K. Nakajima, S. Aizawa, and S. Funahashi, *Bull. Chem. Soc. Jpn.*, **68**, 2293 (1995).

5) a) M. Nakamura, *Inorg. Chim. Acta*, **161**, 73 (1989); b) M. Nakamura, *Bull. Chem. Soc. Jpn.*, **68**, 197 (1995).

6) D. A. Summerville, R. D. Jones, B. M. Hoffman, and F. Basolo, *J. Am. Chem. Soc.*, **99**, 8195 (1977).

7) G. M. Sheldrick, "SHELXS-86, Program for Crystal Structure Determination," University of Göttingen, Germany (1986).

8) S. R. Hall, H. D. Flack, and J. M. Stewart, "Xtal 3.2, Program for X-Ray Crystal Structure Analysis," Universities of Western Australia, Geneva and Maryland (1992).

9) W. C. Hamilton, *Acta Crystallogr.*, **18**, 502 (1965).

10) M. Momenteau, W. R. Scheidt, C. W. Eigenbrot, and C. A. Reed, *J. Am. Chem. Soc.*, **110**, 1207 (1988).

11) W. R. Scheidt and Y. J. Lee, *Struct. Bonding*, **64**, 1 (1987).

12) Y. Zhang, W. A. Hallows, W. J. Ryan, J. G. Jones, G. B. Carpenter, and D. A. Sweigart, *Inorg. Chem.*, **33**, 3306 (1994).

13) A. Takenaka, Y. Sasada, E. Watanabe, H. Ogoshi, and Z. Yoshida, *Chem. Lett.*, **1972**, 1235.

14) D. K. Geiger, Y. J. Lee, and W. R. Scheidt, *J. Am. Chem. Soc.*, **106**, 6339 (1984).

15) W. R. Scheidt, S. R. Osvath, and Y. J. Lee, *J. Am. Chem. Soc.*, **109**, 1958 (1987).

16) W. R. Scheidt, J. F. Kirner, J. L. Hoard, and C A Reed, *J. Am. Chem. Soc.*, **109**, 1963 (1987).

17) M. K. Safo, G. P. Gupta, F. A. Walker, and W. R. Scheidt, *J. Am. Chem. Soc.*, **113**, 5497 (1991).

18) O. Q. Munro, H. M. Marques, P. G. Debrunner, K. Mohanrao, and W. R. Scheidt, *J. Am. Chem. Soc.*, **117**, 935 (1995).

19) W. R. Scheidt, *J. Am. Chem. Soc.*, **96**, 90 (1974).

20) P. N. Dwyer, P. Madura, and W. R. Scheidt, *J. Am. Chem. Soc.*, **96**, 4815 (1974).

21) D. M. Collins, R. Countryman, and J. L. Hoard, *J. Am. Chem. Soc.*, **94**, 2066 (1972).

22) W. R. Scheidt and D. M. Chipman, *J. Am. Chem. Soc.*, **108**, 1163 (1986).

23) a) G. M. Jameson, G. A. Rodley, W. T. Robinson, R. R. Gagne, C. A. Reed, and J. P. Collman, *Inorg. Chem.*, **17**, 850 (1978); b) G. B. Jameson, F. S. Malinaro, J. A. Ibers, J. P. Collman, J. I. Brauman, E. Rose, and K. S. Suslick, *J. Am. Chem. Soc.*, **102**, 3224 (1980).

24) D. G. Oakenfull and W. P. Jencks, *J. Am. Chem. Soc.*, **93**, 178 (1971).

25) M. S. A. Hanza and J. M. Pratt, *J. Chem. Soc., Dalton Trans*, **1994**, 1367.

26) W. P. Jencks and J. Carriuolo, *J. Biol. Chem.*, **234**, 1272 (1959).

27) B. Lenarcik and B. Barszcz, *J. Chem. Soc., Dalton Trans.*, **1980**, 24.

28) J. R. Chipperfield, in "Advances in Linear Free Energy Relationship," ed by N. B. Chapman and J. Shorter, Plenum, London (1972), p. 321.

29) F. A. Walker, *J. Am. Chem. Soc.*, **95**, 1150 (1972).

30) M. S. A. Hanza and J. M. Pratt, *J. Chem. Soc., Dalton Trans.*, **1993**, 1647.

31) F. A. Walker, M.-W. Lo, and M. T. Ree, *J. Am. Chem. Soc.*, **98**, 5552 (1976).